Pergamon

PII: S0042-6989(96)00305-7

Vision Res., Vol. 37, No. 11, pp. 1459–1477, 1997

Printed in Great Britain
0042-6989/97 $17.00 + 0.00

Nonlinear Preprocessing in Short-range Motion

ETHAN TAUB,* JONATHAN D. VICTOR,†‡ MARY M. CONTE†

Received 23 February 1996; in revised form 24 July 1996

The phenomenon of non-Fourier motion (visually perceived motion that cannot be explained simply on the basis of the autocorrelation structure of the visual stimulus) is well recognized, and is generally considered to be due to nonlinear preprocessing of the visual stimulus prior to a stage of standard motion analysis. We devised a sequence of novel visual stimuli in which the availability of a motion stimulus depends on the nature of the nonlinear preprocessing: an *n*th order stimulus P_n will generate a perception of motion if it is preprocessed by a nonlinearity of polynomial order *n* or greater, but not if preprocessed by a nonlinearity of polynomial order less than *n*. We found that unambiguous motion direction was perceived for P_2, P_3, and P_4, but not for higher-order stimuli, and we measured the contrast thresholds for direction discrimination with superimposed noise. We found that an asymmetric compressive nonlinearity can, in a unified fashion, account for these results, while a purely quadratic nonlinearity or a rectification of the form $T(p) = |p|$ cannot. We compared velocity discrimination judgements for second-order non-Fourier stimuli (P_2) with standard drifting gratings. Although velocity comparisons were veridical, uncertainties were greater for the non-Fourier stimuli. This could be reproduced by substituting a Fourier grating with superimposed noise for the non-Fourier grating. These findings are consistent with a single pathway which processes both Fourier and non-Fourier short-range motion, and are discussed in the context of other investigations which have been interpreted as demonstrating separate pathways. © 1997 Elsevier Science Ltd.

Motion analysis Non-Fourier motion

INTRODUCTION

Standard models of motion extraction, based on autocorrelation (e.g., Reichardt, 1961; van Santen & Sperling, 1984), Fourier analysis (e.g., Heeger, 1987), or detection of gradients (e.g., Sobey & Srinivasan, 1991), are sufficient to account for the perception of motion in many, but not all, stimuli that are perceived as moving. The existence of exceptional stimuli, so-called non-Fourier motion stimuli, implies that an elaboration of standard motion models is required. Many psychophysical experiments have been interpreted as implying that independent pathways must exist in the visual system for the perception of Fourier and non-Fourier motion stimuli. Nevertheless, a number of investigators have proposed that these two mathematically distinct types of stimuli can be perceived by a single pathway containing an early nonlinearity. In this paper, we discuss the nature of standard motion models and of Fourier and non-Fourier motion stimuli, and present new data obtained in our laboratory with a novel class of stimuli—"higher-order non-Fourier motion stimuli". Although some models of a separate non-Fourier pathway would appear to require yet a third pathway to account for the perception of motion elicited by these stimuli, we show that our data are in accord with the parsimonious hypothesis of a single pathway. Previously reported data that might appear to require independent processing of Fourier and non-Fourier motion are re-examined, and it is shown that a single pathway can account for these data as well.

STANDARD MOTION ANALYSIS

The velocity of an object is a measurable physical property, but the problem of determining velocity from a visual stimulus is not well-posed. When confronted with a visual stimulus that can be generated by two or more different configurations of moving objects, the visual system has no foolproof way to determine which configuration is the true (physical) one. The familiar barber-pole image, for example, might be generated by an oblique grating moving vertically or horizontally, or even diagonally (Fig. 1). The tendency of an observer to perceive the stripes as moving up the pole, i.e., along the long axis of the aperture through which they are seen, is a result of the way the visual system solves the "aperture problem". More generally, ambiguous stimuli serve as strong tests of models for visual motion analysis because of the multiplicity of *a priori* possible perceptions.

The problem of determining velocity, though not well posed, is readily formalized for our requirements. Formally, a dynamic visual stimulus may be described

*Harvard Medical School, Cambridge, MA 02138, U.S.A.
†Department of Neurology and Neuroscience, Cornell University Medical College, 1300 York Avenue, New York, NY 10021, U.S.A.
‡To whom all correspondence should be addressed.

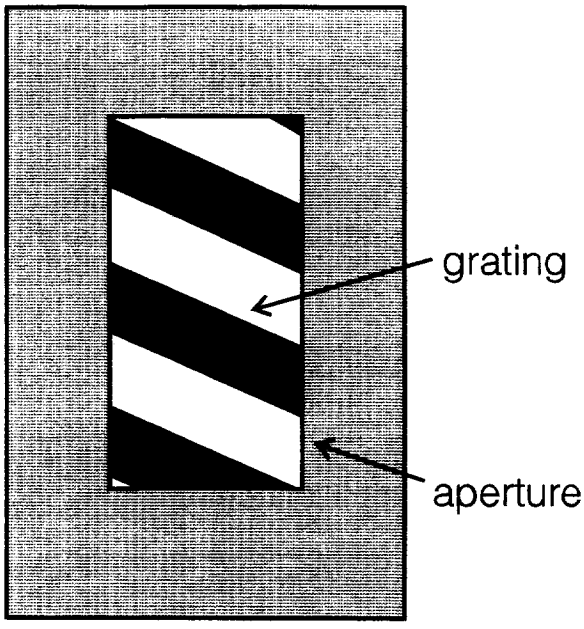

FIGURE 1. The barber-pole illusion. An oblique grating moving behind an elongated aperture appears to be moving in the direction of the long axis of the aperture.

by a function $I(x_1, x_2, t)$, the luminance at retinal location (x_1, x_2) at time t. (The present treatment ignores color and depth.) We will find it useful to rewrite I as

$$I(x_1, x_2, t) = I_0[1 + cP(x_1, x_2, t)], \quad (1)$$

where I_0 is the background luminance, P describes the spatiotemporal stimulus pattern, and c is the contrast. P, unlike I, can take both positive and negative values and is, by convention, normalized to have a maximum deviation of 1 (so that the maximum contrast is c). The visual system is required to perform a computation on P that yields a planar velocity $\mathbf{v} = (v_1, v_2)$ if the stimulus is indeed the image of a rigid object moving at velocity $\mathbf{v}$. A number of different algorithms have been proposed that might perform this task. Our goal is to determine the form of the algorithm used by the visual system, and ultimately, to arrive at a neuroanatomic and neurophysiologic understanding of the visual structures that carry out this algorithm.

How can motion be detected from the stimulus function P? As a simple case, consider a full-field visual stimulus that moves rigidly at a constant velocity $\mathbf{v} = (v_1, v_2)$. This means that for any x_1, x_2, t, and time interval Δt,

$$P(x_1, x_2, t) = P(x_1 + v_1\Delta t, x_2 + v_2\Delta t, t + \Delta t). \quad (2)$$

We now ask what computations can be performed on P that will yield $\mathbf{v}$. We also want our computation to yield $\mathbf{v}$ if condition (2) is "nearly" true, in some sense. One family of possible solutions starts by computing the autocorrelation of P, which is defined as

$$A(x_1, x_2, t) = \langle P(x_1', x_2', t')P(x_1' - x_1, x_2' + x_2, t' + t)\rangle \quad (3)$$

where $\langle\ \rangle$ indicates an average over space (x_1' and x_2') and time (t').

If condition (2) is met for velocity $\mathbf{v}$, then A takes on its maximal value, $\langle P(x_1', x_2', t')^2 \rangle$, at all points of the form (v_1t, v_2t, t). The task of detecting motion and finding $\mathbf{v}$ thus becomes the task of detecting a line of constant values of $A(x_1, x_2, t)$. The motion extraction models of Reichardt (1961) and van Santen & Sperling (1984) are autocorrelational models of this type.

Another approach toward detecting motion begins with a Fourier transformation. The information contained in the stimulus function P may be represented in another way by its Fourier transform, $\hat{P}$, which is defined as

$$\hat{P}(k_1, k_2, \omega) = \iiint e^{-i(k_1x_1 + k_2x_2 + \omega t)}P(x_1, x_2, t)\, dx_1\, dx_2\, dt. \quad (4)$$

Here, $\hat{P}(k_1, k_2, \omega)$ represents the contribution to the visual stimulus made by its Fourier component at spatial frequency $\mathbf{k} = (k_1, k_2)$ and temporal frequency ω. The Fourier components of the visual stimulus are drifting sinusoidal gratings; the Fourier component corresponding to $\mathbf{k}$ and ω is oriented perpendicular to $\mathbf{k}$ and appears to move in the direction of $-\mathbf{k}$ with velocity $\omega\mathbf{k}/|\mathbf{k}|^2$. The qualification "appears to" is necessary, because any additional movement of the grating parallel to its bars is equally consistent with this visual stimulus and therefore cannot be detected. That is, any drifting sinusoidal grating is compatible with a wide range of motion velocities. The gratings that are compatible with velocity $\mathbf{v}$ are precisely those that satisfy $\mathbf{k} \cdot \mathbf{v} + \omega = 0$. These are the gratings for which (k_1, k_2, ω) lies on the plane through the origin perpendicular to the line of points (v_1t, v_2t, t). The task of computing $\mathbf{v}$ from P is therefore the task of identifying a plane which contains all points (k_1, k_2, ω) for which $\hat{P}(k_1, k_2, \omega)$ is nonzero. The motion perception model of Heeger (1987) is a Fourier model of this type.

Autocorrelational motion models are equivalent to Fourier motion models that ignore phase. This is so because of the relation between $\hat{P}$ and $\hat{A}$, the Fourier transform of A:

$$\hat{A}(k_1, k_2, \omega) = |\hat{P}(k_1, k_2, \omega)|^2. \quad (5)$$

That is, $\hat{A}$ (and hence A) can be obtained from $\hat{P}$ by a calculation that ignores phase. The quantity $\hat{P}|(k_1, k_2, \omega)|^2$ is a real number corresponding to the energy of the Fourier component of the stimulus at the spatiotemporal frequency (k_1, k_2, ω). Motion models based on a computation of the autocorrelation A, or, equivalently, the distribution of Fourier energies $|\hat{P}(k_1, k_2, \omega)|^2$, are called "standard" or "first-order" motion models, in the terminology of Chubb & Sperling (1988).

NON-FOURIER MOTION

We have seen that standard motion analysis provides a framework to understand the computation of velocity from visual stimuli. Standard motion analysis cannot, however, account for the perception of motion in *all* stimuli that are seen as moving. The exceptional stimuli have been called "second-order" or "non-Fourier" motion

stimuli (Chubb & Sperling, 1988). We will use the term "non-Fourier" for visual stimuli which elicit the perception of motion, but for which the motion is inaccessible to standard motion analysis. We will use the terms "second-order", "third-order", and "fourth-order" for particular classes of non-Fourier stimuli, in a sense that will be defined. [Our use of the term "second-order" coincides with that of Chubb & Sperling (1988,1989), but our use of the term "third-order" (Taub & Victor, 1993) differs from that of Lu & Sperling (1995a,b), who used the term to characterize motion stimuli based on their perceptual features, rather than on their statistical properties.]

Our second-order non-Fourier motion stimulus is a modified drifting sinusoidal grating constructed from unit-sized checks. The value of the stimulus function P_2 at each check is determined by multiplying the grating by either +1 or −1, with the value chosen randomly at each check. Thus, for integer values of x_1 and x_2,

$$P_2(x_1, x_2, t) = (-1)^{R(x_1, x_2)}\cos(k_1'x_1 + k_2'x_2 + \omega' t). \quad (6)$$

where $R(x_1, x_2)$ is chosen randomly and independently from {0, 1} at each pair of integers (x_1, x_2). Equation (6) will be more readily generalizable in what follows if we rewrite it equivalently as

$$P_2(x_1, x_2, t) = \cos(k_1'x_1 + k_2'x_2 + \omega' t + \pi R(x_1, x_2)). \quad (7)$$

All checks are modulated sinusoidally in time at the frequency ω'. An instantaneous snapshot of this stimulus, shown in Fig. 2, resembles a randomly colored checkerboard modulated by a sine wave, so that a grating of gray bars appears. With this temporal modulation, the gray bars appear to drift across the screen.

Standard motion analysis cannot account for the perception of motion in this stimulus. The key observation is that the random choice of $R(x_1, x_2)$ forces the autocorrelation of P_2 to be zero:

$$\begin{aligned} A_2(x_1, x_2, t) &= \langle P_2(x_1', x_2', t')P_2(x_1' + x_1, x_2' + x_2, t' + t)\rangle \\ &= \langle (-1)^{R(x_1', x_2')}(-1)^{R(x_1' - x_1, x_2' - x_2)}\cos(k_1'x_1' + k_2'x_2' + \omega' t')\cos(k_1'(x_1' + x_1) - k_2'(x_2' + x_2) + \omega'(t' + t))\rangle. \\ &= 0 \end{aligned} \quad (8)$$

unless $x_1 = 0$ and $x_2 = 0$, because $R(x_1' + x_1, x_2' + x_2)$ and $R(x_1', x_2')$ are independent. For $x_1 = 0$ and $x_2 = 0$, the autocorrelation function reduces to that of a grating: $A_2(0, 0, t) = \cos(\omega' t)/2$.

It follows from Eq. (5) that the Fourier motion energy $|\hat{P}_2(k_1, k_2, \omega)|^2$ is nonzero only at points where $\omega = \pm\omega'$, and its values at these points are independent of k_1, k_2, and ω. Thus, $|\hat{P}_2(k_1, k_2, \omega)|^2$ contains an equal amount of energy in opposite directions, and hence no net motion energy.

Until now, we have ignored any visual processing which might precede the extraction of motion energy. However, to the extent that we can characterize the "front end" as a linear filter, the above argument remains valid. Passing the stimulus P_2 through a linear transformation L will have the effect of multiplying each Fourier component $\hat{P}_2(k_1, k_2, \omega)$ of the stimulus by a complex number [the value of the transfer function $\hat{L}(k_1, k_2, \omega)$], and will thus not introduce any new nonzero Fourier components into $|\hat{P}_2(k_1, k_2, \omega)|^2$.

While standard motion analysis cannot account for the *global* motion of the P_2 stimulus, it can account for *local* motion in small areas of the stimulus. When the P_2 stimulus is viewed in a small region [less than one wavelength $(2\pi/k')$ in width], it no longer appears to be a drifting grating. Rather, it looks like temporally varying random speckle, and local motion in either direction is sometimes seen. The average in Eq. (8) is guaranteed to be zero only if computed globally. Over restricted ranges of time and space, an empiric measurement of the autocorrelation $A_2(x_1, x_2, t)$ may be nonzero. However, unless $x_1 = 0$ and $x_2 = 0$, these estimates will fluctuate evenly around zero. This estimate of the autocorrelation may thus provide a nonzero motion signal, but one of random direction. Thus, a subject viewing the entire stimulus and using standard motion analysis would be expected to perceive randomly directed local motion. It is only the unidirectional, global motion of the P_2 stimulus that cannot be perceived with standard motion analysis. In our psychophysical experiments on P_2 and other non-Fourier motion stimuli, we have avoided the confounding effect of local motion by measuring thresholds for global direction discrimination rather than detection of motion as such.

To account for the perception of steady, unambiguous global motion in P_2 (and other non-Fourier motion stimuli), an extension of the standard model is required. The standard motion model can be schematically summarized by

$$P \longrightarrow \textit{linear filter } L \longrightarrow L[P] \longrightarrow \textit{standard motion analysis} \longrightarrow \textit{velocity } \mathbf{v}. \quad (9)$$

We suggest [as did Chubb & Sperling (1989)] that the visual stimulus is subjected to a *nonlinear* transformation before undergoing standard motion analysis:

$$P \longrightarrow \textit{linear filter } L \longrightarrow L[P] \longrightarrow \textit{nonlinear transformation } T \longrightarrow T[L[P]] \longrightarrow \textit{standard motion analysis} \longrightarrow \textit{velocity } \mathbf{v}. \quad (10)$$

This suggestion is biologically plausible, because strong nonlinearities early in the visual system are known to exist. For example, a defining property of a Y cell is that it increases its firing rate in response to the introduction of a pattern into its receptive field and to its withdrawal. This must be the result of nonlinear

spatial summation (Enroth-Cugell & Robson, 1966; Hochstein & Shapley, 1976). As another example, many cells in the primary visual cortex have little or no maintained discharge. As a result, they act as rectifiers. An on-center cell will increase its firing rate (from zero to some positive value) when confronted with a bright center and a dark surround, but cannot decrease its firing rate by an equal amount when confronted with the inverse stimulus. In principle, photoreceptor nonlinearities might also contribute to T, but such nonlinearities, which are smooth functions in the neighborhood of a contrast of zero, are unlikely to account for our findings (see section entitled "Estimation of the form of the nonlinearity T").

The nonlinear transformation T is critical to the emergence of unambiguous motion energy in a non-Fourier stimulus. For the second-order stimulus P_2 of Eqs (6) and (7), any nonlinear transformation that eliminates the cancellation of the factors ± 1 in Eq. (8) will lead to a nonzero value of the autocorrelation A_2, and thus, provide a nonzero input to standard motion analysis. Thus, full-wave rectification, $(T(p) = |p|)$, half-wave rectification $[T(p) = |p|$ for $p \geq 0$ and 0 for $p < 0]$, and a squaring transformation $(T(p) = p^2)$ would all reveal unambiguous motion in P_2. Because the squaring transformation is analytic, its effect is readily calculated explicitly. Initially, we ignore L:

$$T[P_2](x_1, x_2, t) = \cos^2(k_1'x_1 + k_2'x_2 + \omega' t + R(x_1, x_2)\pi)$$

$$= \frac{1}{2} + \frac{1}{2}\cos(2k_1'x_1 + 2k_2'x_2 + 2\omega' t). \qquad (11)$$

$T[P_2]$ thus contains a sinusoidal grating at spatiotemporal frequency $(2k_1', 2k_2', 2\omega')$, and will therefore be accessible to standard motion analysis. Note that such a grating has the same speed as the original grating from which the stimulus P_2 was derived, but with twice the spatial and temporal frequency. This accords well with the perception of moving gray bars: the bars are at the zeroes of a sinusoid of spatiotemporal frequency (k_1', k_2', ω'), and there are thus two bars perceived in P_2 for every

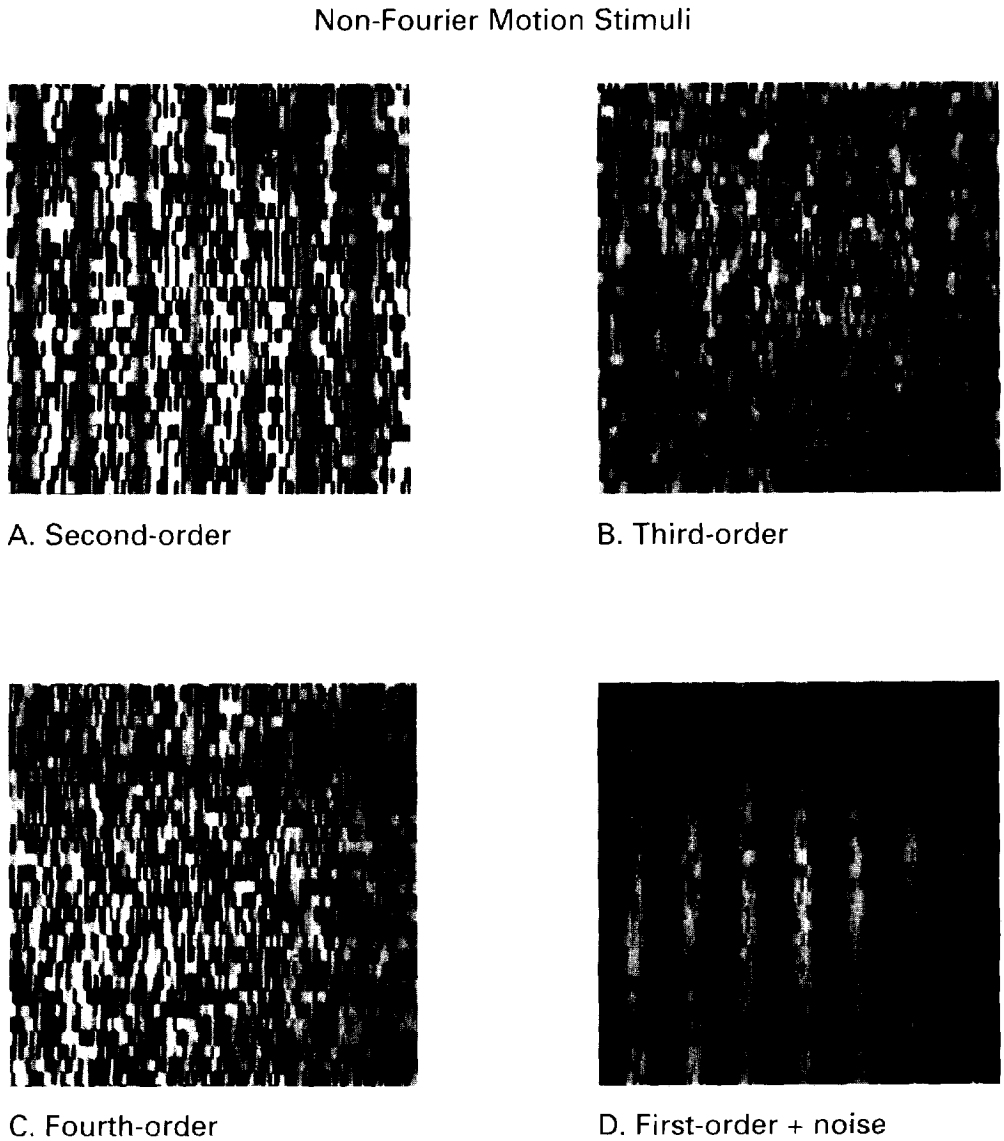

FIGURE 2. Individual frames of the motion stimuli used in these experiments.

period of the underlying sinusoid. The presence of a nontrivial initial filter L complicates the analysis but has no major effect on the conclusions: $T[L[P_2]]$ will be dominated by a sinusoid at $(2k_1', 2k_2', 2\omega')$ whose amplitude is determined by the behavior of L at the temporal frequency ω' and spatial frequencies comparable to the pixel frequency.

Although the idea that $T(p) = p^2$ is attractive from the standpoint of analytic simplicity, there are many things that it cannot account for. If the motion pathway were the only short-range analysis pathway present, then stimuli in which a standard grating shifted by one-quarter of a cycle on each frame would appear ambiguous—this is decidedly not the case (Nakayama & Silverman, 1985). On the other hand, if the motion pathway [equation (10)] were in parallel with a standard motion analysis pathway without an initial nonlinearity [equation (9)], then the many striking similarities in the processing of short-range Fourier and non-Fourier motion (Turano & Pantle, 1989; Turano, 1991; Victor & Conte, 1992b; Witt *et al.*, 1994; Lu & Sperling, 1995a; Ledgeway & Smith, 1995a,b) would require explanation. For these reasons, we pursue the idea that a single motion pathway of the scheme [equation (10)], with an asymmetric nonlinearity T, might account for observations concerning both Fourier and non-Fourier motion. Half-wave rectification, transformations of the form $T(p) = p + a_2 p^2$, and many other functional forms are potential candidates for this asymmetric nonlinearity. Experiments 1 and 2 constrain these possibilities, and attempt to define the form of T. Experiments 3 and 4 compare velocity judgments for Fourier and non-Fourier gratings, to determine whether the findings are consistent with a single-pathway model.

METHODS

Stimulus delivery

Motion stimuli were generated on a custom-designed visual stimulator (modified from Milkman *et al.*, 1980) interfaced to a PDP 11/73 computer. Stimuli were presented on a Tektronix 608 monitor (256×256 pixels covering 8.8×8.8 cm), which provides a monochromatic display of mean luminance 150 cd/m^2 at 270.3 Hz. We compensated for the nonlinear voltage–luminance characteristic of the CRT with a look-up table derived from photocell measurements. With this compensation, stimulus luminance was linear (as a function of desired stimulus value) to within approximately 1% over the entire range of values used.

Stimuli were composed of checks which measured 1 pixel (horizontal) by 4 pixels (vertical) on the CRT. At our viewing distance of 57 cm, checks measured 0.034×0.138 deg. (Checks are larger, for demonstrative purposes, in the still photograph, in Fig. 2.) Gratings were vertically oriented (i.e., $k_2' = 0$). Spatial frequency [$k_1'/2\pi$ for a standard grating, k_1'/π for the second-order non-Fourier grating of Eq. (6), or $nk_1'/2\pi$ for the n-th order non-Fourier grating of Eq. (12)] was 1 c/deg.

Five subjects, ranging in age from 20 to 38 years, participated in these experiments. All were normal observers with visual acuity corrected to 20/20. Subjects were instructed to fixate on a small dot in the middle of the display, but eye movements were not measured.

Display nonlinearities

It is well known that CRTs are subject to nonlinearities that cannot readily be corrected via a look-up table (Pelli & Zhang, 1991; Naiman & Makous, 1992). We measured the effect of these spatial and dynamic nonlinearities by comparing the monitor's light output during display of a uniform field set to background with its light output during display of square-wave gratings, for nominal contrasts of up to 0.5. For 128 cycle/screen gratings parallel to the raster (which required changes in the intensity signal as each raster line is scanned), there was less than a 1% change in the mean luminance. For gratings perpendicular to the raster at 128 cycles/screen (which required changes of the intensity signal as each pixel is scanned), there was an 8% decrease in the mean luminance at a contrast of 0.5, and a 3% decrease at a contrast of 0.25. The extent of this nonlinearity is expected to be proportional to spatial frequency (Naiman & Makous, 1992), so that for the check sizes (4 pixels along the "fast" axis) and contrasts (r.m.s. at most 0.5, typically 0.25) used, the dynamic nonlinearity was always less than 2%, and typically less than 1%. It is unlikely (see section entitled "Estimation of the form of the nonlinearity T") that these errors or look-up table inaccuracies contributed either to the detection of motion in the non-Fourier stimuli used or to modelling errors.

Psychophysical methods

Contrast thresholds for direction discrimination were determined by a two-alternative forced-choice staircase method. Stimuli were presented for 1 sec, and subjects were asked to determine whether the dominant direction of motion was leftward or rightward. After two preliminary reversals with step sizes of 0.3 log units, the geometric means of eight reversals with step sizes of 0.05 log units (two correct answers in a row to decrease contrast, one incorrect answer to increase contrast) were averaged to estimate a threshold contrast for 71% correct performance. To avoid the possibility that subjects were cued by initial feature location, final feature location, or distance travelled, the initial phase of the grating was fully randomized, and spatial frequency, velocity, and duration were jittered by 10% about their nominal values.

Velocity judgments were assessed by a method of constant stimuli. Stimuli were presented sequentially for 1 sec each in pairs, with the first stimulus designated as the "standard" and the second stimulus designated as the "probe". Subjects were asked to determine whether the probe stimulus velocity was faster or slower than that of the standard. In each presentation, spatial phase was randomized, duration was jittered by 25%, and spatial frequency was jittered by 20%. Velocity was jittered by 20%, but the same jittered values were applied to standard and probe stimuli within the same trial. All

possible (standard velocity, probe velocity) combinations were presented in randomized order within one block, and 18–20 blocks of data were collected.

In both series of experiments, subjects were allowed practice trials with feedback until performance had stabilized. During data collection, no feedback was given.

RESULTS

Experiment 1: Motion thresholds for second-order stimuli

Second-order non-Fourier motion stimuli were generated according to Eq. (6) and presented to three subjects (JV, MC and ET) for pattern velocities ranging from 1 to 16 deg/sec (with 10% jitter). With no added noise, subjects correctly gave the direction of motion at relatively low contrast levels (Fig. 3)—though not as low as those sufficient for detection of a first-order (Fourier) stimulus (see Fig. 4 below).

We also measured direction discrimination thresholds in the presence of noise. For these experiments, the "noise" (defined precisely below) essentially consisted of sinusoidal contrast modulation of each pixel, with the phase of the modulation at each pixel chosen at random. Noise was added to the second-order non-Fourier stimuli by alternating noise frames with frames consisting of the non-Fourier motion stimulus, and adjusting the contrasts of the individual frames to compensate for the 1:1 interleave. As shown in Fig. 3, the addition of noise elevated the threshold contrast for direction discrimination. The amount of elevation was similar across subjects and approximately proportional to the amount of added noise.

This experiment shows that second-order non-Fourier motion stimuli are seen as moving in an unambiguous direction, even though they necessarily contain areas of randomly appearing, randomly directed local first-order motion. It follows that standard motion analysis cannot be the only operative mechanism in motion processing, and that an initial nonlinearity T [Eq. (10)] is required.

Experiment 2: Motion thresholds for higher-order non-Fourier motion stimuli

As pointed out above, the perception of motion in the second-order non-Fourier motion stimulus could be accounted for by supposing that the nonlinear transformation T is of the form $T(p) = p + a_2p^2$. We now test this hypothesis by defining a new non-Fourier motion stimulus P such that $T[L[P]]$ (for $T(p) = p + a_2p^2$) is inaccessible to standard motion analysis. If P is nonetheless seen as moving, then the hypothesis that $T(p)$ is quadratic must be rejected.

We define an *nth-order non-Fourier motion stimulus* as one that generates a motion signal on standard motion analysis if it is initially passed through linear filtering and some nonlinear transformation of order n, but does not generate a motion signal if it is passed through a nonlinear transformation of any lower order. The stimuli of Eq. (6) satisfy this definition for $n = 2$, as do the non-Fourier stimuli introduced by Chubb & Sperling (1988, 1989). We now construct higher-order non-Fourier stimuli by generalizing Eq. (7), an equivalent form of Eq. (6), to arbitrary n. Let

$$P_n(x_1, x_2, t) = \cos\left(k_1'x_1 + k_2'x_2 + \omega' t + \frac{(2\pi)}{n}R(x_1, x_2)\right), \tag{12}$$

where $R(x_1, x_2)$ is chosen independently from $\{0, 1, \ldots, n-1\}$ at each check (x_1, x_2).

To show that the stimuli P_n of Eq. (12) do, in fact, meet the definition of nth-order non-Fourier motion stimuli, we show that for all $m < n$, the autocorrelation of any mth-degree polynomial in $P_n(x_1, x_2, t)$ is zero, except at zero spatial disparity. However, since $[P_n(x_1, x_2, t)]^n$ will be shown to have a nonzero Fourier component at

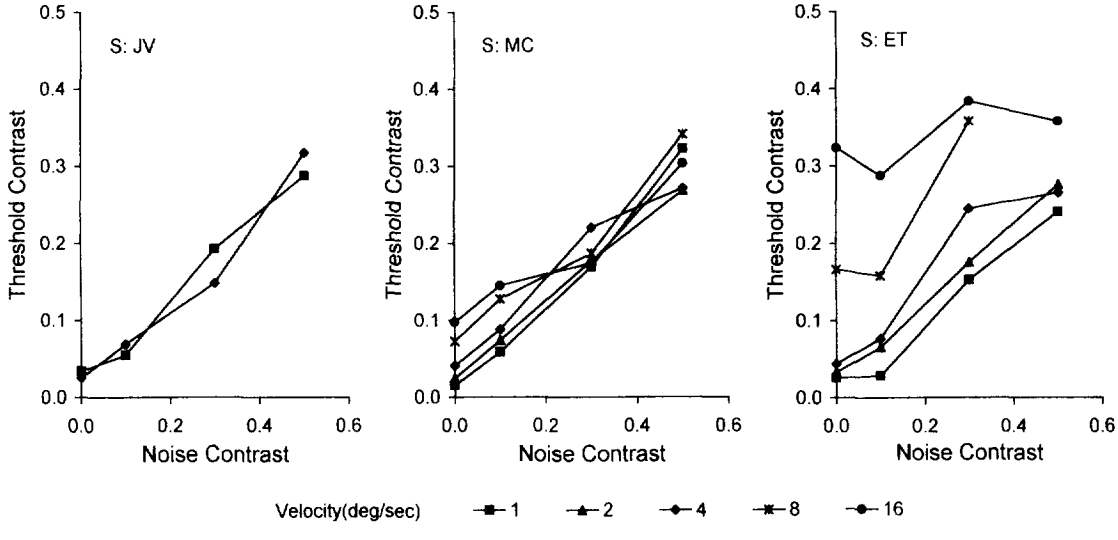

FIGURE 3. Threshold contrast for discrimination of direction of motion for the second-order stimulus P_2 with varying amounts of added noise.

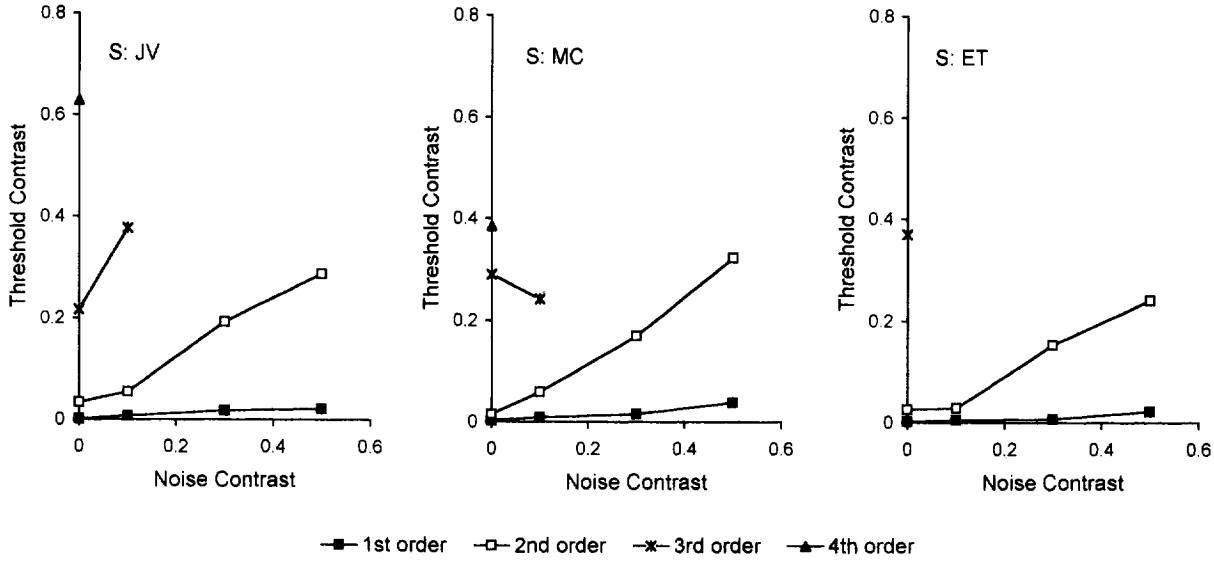

FIGURE 4. Threshold contrast for discrimination of direction of motion for nth-order motion stimuli P_1, P_2, P_3 and P_4, with varying amounts of added noise. Velocity: 4 deg/sec.

spatiotemporal frequency $(nk_1', nk_2', n\omega')$, it will yield a signal on standard motion analysis provided that T is a polynomial with a term of order n.

Let $Q[P_n(x_1, x_2, t)]$ be an mth-degree polynomial in $P_n(x_1, x_2, t)$, and consider the jth-degree term in Q:

$$[P_n(x_1, x_2, t)]^j = \cos^j\left(k_1'x_1 + k_2'x_2 + \omega' t + \frac{2\pi}{n}R(x_1, x_2)\right)$$

$$= \frac{1}{2^j}\left\{\exp\left[\imath\left(k_1'x_1 + k_2'x_2 + \omega' t + \frac{2\pi}{n}R(x_1, x_2)\right)\right]\right.$$

$$\left.+\exp\left[-\imath\left(k_1'x_1 + k_2'x_2 + \omega' t + \frac{2\pi}{n}R(x_1, x_2)\right)\right]\right\}^j. \tag{13}$$

Each term in the binomial expansion of the last expression has a phase offset of the form $2\pi hR(x_1, x_2)/n$, with h in the range $\{-j, -j+2, -j+4, \ldots, j-4, j-2, j\}$. The autocorrelation of $Q[P_n(x_1, x_2, t)]$, which involves products of terms in $Q[P_n(x_1', x_2', t')]$ and $Q[P_n(x_1' + x_1, x_2' + x_2, t' + t)]$ is a cross-product of such expressions, and therefore contains terms with nontrivial phase factors of the form

$$\exp\left[\imath\frac{2\pi}{n}\left(h'R(x_1', x_2') + hR(x_1' + x_1, x_2' + x_2)\right)\right]. \tag{14}$$

where both $|h|$ and $|h'|$ are no greater than the degree m of Q. Provided that x_1 and x_2 are not both zero, the values of $R(x_1', x_2', t')$ and $R(x_1' + x_1, x_2' + x_2)$ are independent and equally distributed among the choices $\{0, 1, \ldots, n-1\}$. Thus, an ensemble-average of any term involving the phase factor is necessarily zero, except where $x_1 = x_2 = 0$. Consequently an m-th order polynomial Q cannot serve as a nonlinear transformation which extracts motion.

On the other hand, if the nonlinear transformation T is a polynomial which contains a term of degree n, then $T[P_n]$ will yield an unambiguous motion signal when subjected to standard motion analysis. From Eq. (13), we find

$$[P_n(x_1, x_2, t)]^n = \cos^n\left(k_1'x_1 + k_2'x_2 + \omega' t + \frac{2\pi}{n}R(x_1, x_2)\right)$$

$$= \frac{1}{2^n}\left\{\exp\left[\imath\left(k_1'x_1 + k_2'x_2 + \omega' t + \frac{2\pi}{n}R(x_1, x_2)\right)\right]\right.$$

$$\left.+\exp\left[-\imath\left(k_1'x_1 + k_2'x_2 + \omega' t + \frac{2\pi}{n}R(x_1, x_2)\right)\right]\right\}^n$$

$$= \frac{1}{2^{n-1}}\cos\left[n\left(k_1'x_1 + k_2'x_2 + \omega' t\right)\right]$$

$$+ \textit{DC-term} + \textit{terms whose phase depends on } R(x_1, x_2). \tag{15}$$

The terms whose phase depends on $R(x_1, x_2)$ will vanish in the computation of the autocorrelation. The DC-term, which is present only if n is even, cannot contribute to a directional motion signal. However, the cosine term, which represents a sinusoid with spatiotemporal frequency $(nk_1', nk_2', n\omega')$, will remain. The above reasoning is valid even if a linear filter L is applied to the stimulus P_n prior to application of the local nonlinearity T, because L will neither create signal components at new temporal frequencies, nor introduce new kinds of spatial interactions into products of expressions similar to Eq. (13).

This shows that P_n, as defined by Eq. (12), meets our definition of an nth-order non-Fourier motion stimulus: it will yield an unambiguous motion signal on standard motion analysis if initially acted upon by a nonlinearity of order n, but will not if acted on by a nonlinearity of any lower order. In the limit that n is infinite, P_n becomes independent sinusoidal modulation at each check, with the phase at each check chosen randomly and indepen-

dently. Given our empirical finding (see below) that motion in P_n is not perceptible for $n \geqslant 5$, we used P_8 as an approximation to random-phase noise in these experiments.

Note that in Eq. (15) the coefficient of the cosine term in $[P_n(x_1, x_2, t)]^n$ is $1/2^{n-1}$. Thus, the amount of energy in its autocorrelation at the spatiotemporal frequency $(nk_1', nk_2', n\omega')$ is $[1/2^{n-1}]^2$, which approaches zero rapidly with increasing n. It is therefore expected that nth-order non-Fourier motion will not be visible for sufficiently large n because, even if the motion mechanism contains a nonlinearity of order n, the Fourier motion energy of the transformed stimulus is likely to be subthreshold. Experiment 1 shows that P_2 produces an unambiguous motion signal even for relatively small contrasts. We next ask whether, for higher values of n, P_n produces an unambiguous motion signal, and if so, how the threshold contrast for direction discrimination depends on noise contrast.

Higher-order non-Fourier motion stimuli were generated according to Eq. (12) and presented to subjects JV, MC and ET. In preliminary two-alternative forced-choice testing at a contrast of 1.0, all subjects saw unambiguous motion for P_3 and P_4, while no subject performed above chance for P_n, $n = 5$, 6, 7 or 8. The appreciation of unambiguous motion for P_3 and P_4 was spontaneous, and did not require feedback or training. As in Experiment 1, we next determined thresholds for direction discrimination for the third- and fourth-order stimuli in the presence of noise.

Results are shown in Fig. 4 for a drift velocity of 4 deg/sec. Third-order stimuli, like second-order stimuli, are seen as moving by all observers, though at higher contrast thresholds. Fourth-order stimuli are seen as moving at only the highest contrast levels—the contrast threshold for direction discrimination is on the order of 0.5 for all observers. Thresholds in the presence of noise could not be reliably determined for P_4, because the maximum contrast available in an interleaved display was 0.5, which was comparable to the direction discrimination thresholds for these stimuli. Nevertheless, it is noteworthy that the fourth-order stimuli are perceived as moving at all, given the attenuation of motion energy by a factor of 64 $(= [1/2^{4-1}]^2)$.

It is interesting, but as yet unexplained, that one of the subjects (ET) consistently perceived unambiguous motion in P_4, but this motion was in the reverse of the "veridical" direction. One possibility is that this subject, who had the least experience as a psychophysical observer, was unable to suppress tracking movements, and reported the apparent direction of motion of the edges of the checks.

Estimation of the form of the nonlinearity T

We have shown that transformation T of Eq. (10), the hypothesized early nonlinearity in visual motion processing, cannot be a polynomial of order less than four—if so, non-Fourier motion stimuli of order 4 would not be perceptible as moving. We now derive an estimate of the form of T from the data obtained in Experiments 1 and 2.

Our strategy is as follows. For any stimulus $P(x_1, x_2, t)$ and an assumed form for T, one can calculate: (1) $T[P](x_1, x_2, t)$; (2) the Fourier transform of $T[P](x_1, x_2, t)$; and therefore (3) the Fourier motion energy in $T[P](x_1, x_2, t)$, which is the motion signal that the nonlinearly transformed stimulus presents to the standard motion analyzer in the scheme. We assume that the detection of motion is based on a space–time average of the directional motion energy in $T[P]$. The energy in the Fourier transform of $T[P]$ which does not contribute to a directional motion signal is noise from the point of view of the motion analyzer.

If a single pathway such as the scheme [equation (10)] is correct, then (for stimuli of comparable spatial and temporal structure), contrast thresholds for direction discrimination should depend only on the directional motion energy and noise in $T[P](x_1, x_2, t)$, and not on the order of stimulus (i.e., not on P_1 vs P_2 vs P_3 etc.) nor on whether the noise was explicitly added to the stimulus, or a consequence of the R-dependent terms in Eq. (15). It is important to note that the signal and noise in the transformed stimulus $T[P]$ depend in a complex (and not always intuitive) manner on the signal and noise in the original stimulus P, as well as on the nature of the transformation T. Since our estimation of T is essentially based on "silent substitution" of Fourier and non-Fourier stimuli, it is not likely to be influenced by processes such as large-area pooling of local motion signals or probability summation.

To implement this strategy, we assumed that the nonlinear transformation T was of the form

$$T(p) = \begin{cases} |p|^{\alpha}, & p \geqslant 0, \\ -g|p|^{\alpha}, & p < 0 \end{cases} \quad (16)$$

We kept the number of adjustable parameters in T low so that a good fit to all of the data would provide a strong test of our model. Nevertheless, the two parameters α and g cover many *a priori* reasonable choices for T, including a linear transformation ($\alpha = 1$, $g = 1$), half-wave rectification ($\alpha = 1$, $g = 0$), full-wave rectification ($\alpha = 1$, $g = -1$), squaring ($\alpha = 2$, $g = -1$), and other power laws.

In Fig. 5(A), we present the relationship of the threshold contrast for direction discrimination to noise for subject MC, under the assumption that T is a linear transformation. The square root of the motion energy that reaches the motion analyzer is plotted along the ordinate, and the square root of the noise energy that reaches the motion analyzer is plotted along the abscissa. In this calculation, we have included the residual intensity–voltage nonlinearity in the display due to look-up table errors. Thus, the energy available for standard motion analysis is not exactly zero for P_2, P_3 and P_4. Not surprisingly, data for different kinds of stimuli do not lie along the same curve: direction is consistently detected for the non-Fourier stimuli (P_2, P_3 and P_4) at contrasts for which very little motion energy is available for standard motion analysis. The fact that the thresholds for motion

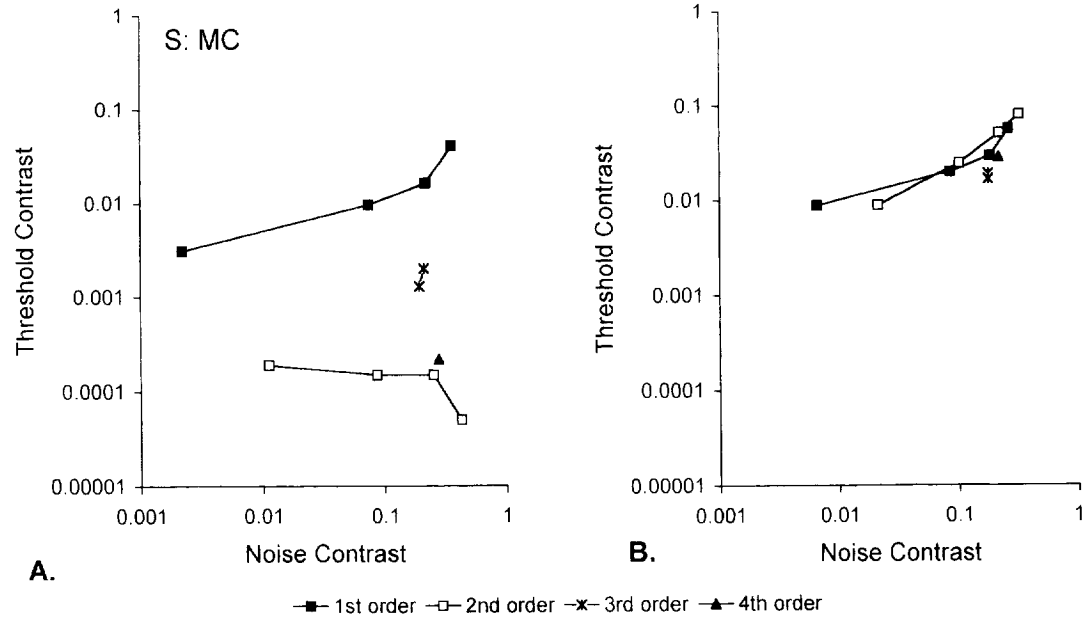

FIGURE 5. (A) Data for subject MC of Fig. 4, plotted in terms of the noise contrast present in the display. (B) Data from (A), plotted in terms of the noise contrast following a nonlinear transformation (see Fig. 6).

detection for these stimuli lie one to two orders of magnitude below the thresholds for P_1 indicates that intensity nonlinearities of the monitor do not contribute to the detection of these stimuli.

We then adjusted T via the parameters α and g of Eq. (16) so that, in a least-squares sense, the threshold contrasts lay on a common line. The transformation T was applied following the empirical residual intensity nonlinearity of the monitor. T affects not only the amount of root-mean-squared motion energy that reaches the motion analyzer (plotted along the ordinate), but also the amount of root-mean-squared noise energy (plotted along the abscissa), and it affects both Fourier and non-Fourier stimuli. Following this transformation, which corresponds to Eq. (16) with $\alpha = 0.72$ and $g = 0.08$, the thresholds for the four stimulus types lie along a common line [Fig. 5(B)]. That is, with this preprocessing stage, the thresholds for detection of non-Fourier and Fourier motion, with or without added noise, can be accounted for on the basis of a common nonlinear transformation and detection mechanism.

Figure 6 shows the nonlinear transformation T derived from the data of Fig. 5. Note that T is a compressive function, and that it treats positive and negative contrasts differently (and thus, can preserve luminance information for standard motion analysis).

A similar analysis (Fig. 7) was performed on data

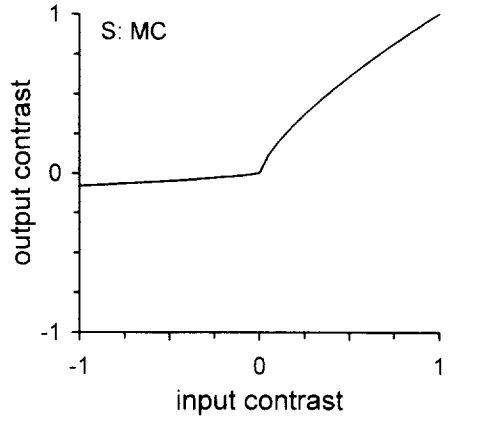

FIGURE 6. The nonlinear transformation T [Eq. (16)] with $\alpha = 0.72$ and $g = 0.08$.

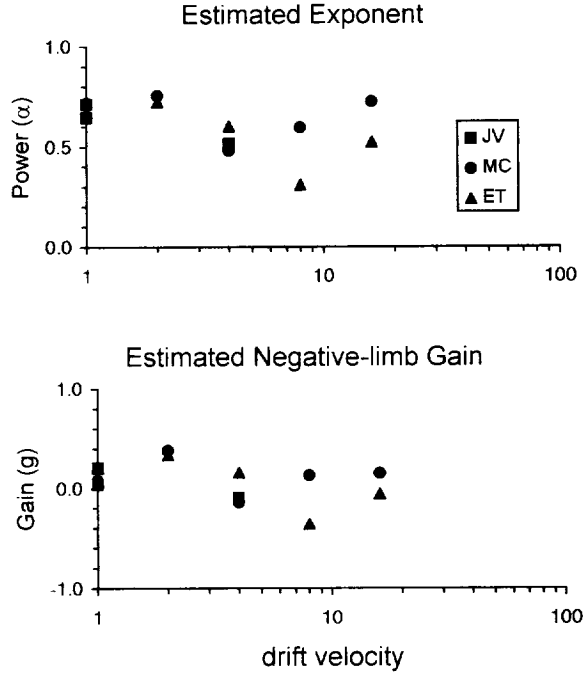

FIGURE 7. Parameters for the nonlinear transformation T [Eq. (16)] estimated from experiments conducted at a range of velocities, across subjects.

obtained in all three subjects and at various pattern velocities, including the P_2 data of Fig. 3. The power α was usually in the vicinity of 0.5 (mean, 0.45; range, 0.25–0.65). The gain for negative contrasts g was usually negative and always had absolute value <0.5 (mean, −0.1638; range, −0.4690 to +0.2185). Although there is some scatter in these values, there is no systematic dependence on velocity or subject. Factors that contribute to this variability probably include uncertainty in the measurement of psychophysical thresholds, and the constraints of the form [equation (16)] of T. Nevertheless, the data clearly exclude a power α near 1, as well as a nonlinearity which is nearly symmetric (g near −1) and nearly antisymmetric (g near 1). Rather, these findings suggest that T may be thought of as partial rectification with a fractional power law intensity–response function, and may be approximated by

$$T(p) = \max(0, p^{0.5}). \quad (17)$$

The analysis so far has not considered a stage L of early linear filtering which precedes the posited nonlinearity T. Although a detailed analysis requires knowledge of the form of L, one can nevertheless understand the effects of linear preprocessing without knowledge of its form. Since all spatiotemporal Fourier components of P_n have the same temporal frequency, the temporal filtering associated with L will simply produce an overall amplitude change and phase shift, and thus not affect on the calculation of directional motion energy and noise energy. The effects of spatial filtering due to L are likely to be more significant. In the extreme situation that L combines values from a large number of nearby pixels, the filtered stimulus will have nearly Gaussian-distributed values, independent of position in the stimulus cycle, and no model can extract the motion signal. More generally, to the extent that L can be viewed as combining luminance values from nearby pixels (whether this combination is additive or subtractive), these nearby, uncorrelated pixels will appear to be a source of noise. As such, the "linearizing" effects (Spekreijse & Oosting, 1970) of this noise will diminish the effectiveness of any nonlinearity in extracting the non-Fourier motion. Consequently, spatial filtering due to L will tend to make T appear more nearly linear. Models which omit explicit consideration of L thus will tend to underestimate the nonlinearity T. That is, our estimates of α and g will be biased towards 1.

Experiment 3: Velocity discrimination for Fourier and non-Fourier stimuli

To remain tenable, the single-pathway hypothesis must account not only for direction-discrimination thresholds, but also for other aspects of motion perception. The next experiment asks whether Fourier and second-order non-Fourier gratings of comparable contrast (Stone & Thompson, 1992), spatial characteristics, and temporal characteristics are perceived as having the same velocity, and whether velocity discrimination thresholds for

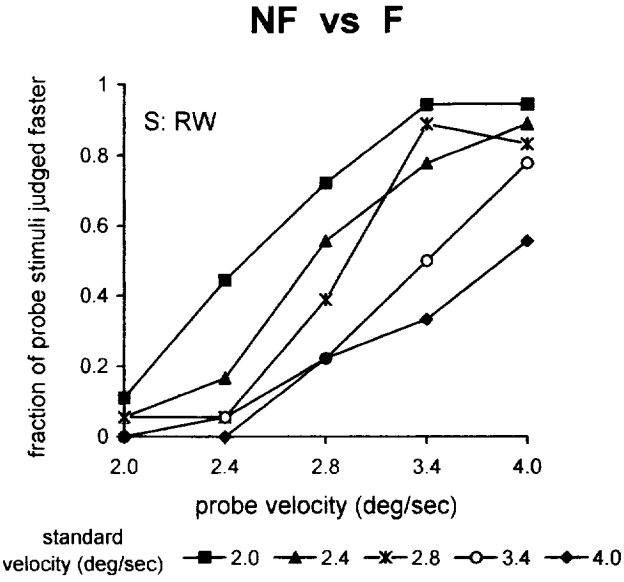

FIGURE 8. Psychometric functions for pairwise velocity comparisons between probe Fourier gratings of five velocities with standard non-Fourier gratings of five velocities, each in the range 2–4 deg/sec. Each was presented at a contrast equal to 10 times its detection threshold (0.041 for the Fourier grating, and 0.106 for the non-Fourier grating). All 25 comparisons were randomly intermixed. Subject: RW.

Fourier and non-Fourier gratings can be accounted for by a single pathway.

Three subjects (MC, NW and RW) participated in this series of experiments. In the first set of experiments, subjects compared Fourier and second-order non-Fourier (P_2) gratings at a nominal spatial frequency of 1 c/deg [$nk_1'/2\pi = 1$ in Eq. (12)]. For this experiment, stimuli were presented at a contrast equal to 10 times the subject's detection threshold for the non-Fourier grating. In each trial, subjects were asked to compare the velocity of two stimuli: a "standard" and a "probe." The 25 kinds of trials (standard and probe stimuli presented at each of five velocities ranging from 2.0 to 4.0 deg/sec) were presented in random order, and responses were accumulated across 18 of these blocks.

Figure 8 illustrates velocity comparison data obtained from subject RW. The fraction of times that the probe (Fourier) stimulus was judged faster than standard (non-Fourier) stimulus, $f(r)$, is a sigmoidal function of the velocity ratio, r. The velocity ratio at which the probe was judged faster exactly half of the time indicates the point of subjectively equal velocities, and the slope of the psychometric function indicates the uncertainty of the velocity comparisons—i.e., the range of probe velocities that is accepted as approximately equal to the standard. These data were fitted to a cumulative normal probability distribution by a least-squares method:

$$f(r, b, \sigma) = \frac{1}{\sqrt{\pi}\sigma} \int_{-\infty}^{\log r} \exp\left[-\left(\frac{u - \log b}{\sigma}\right)^2\right] du \quad (18)$$

In this equation, b is the judgment bias: it is the velocity ratio at which subjectively equal velocities were reported. The uncertainty is expressed by σ, and is essentially a just

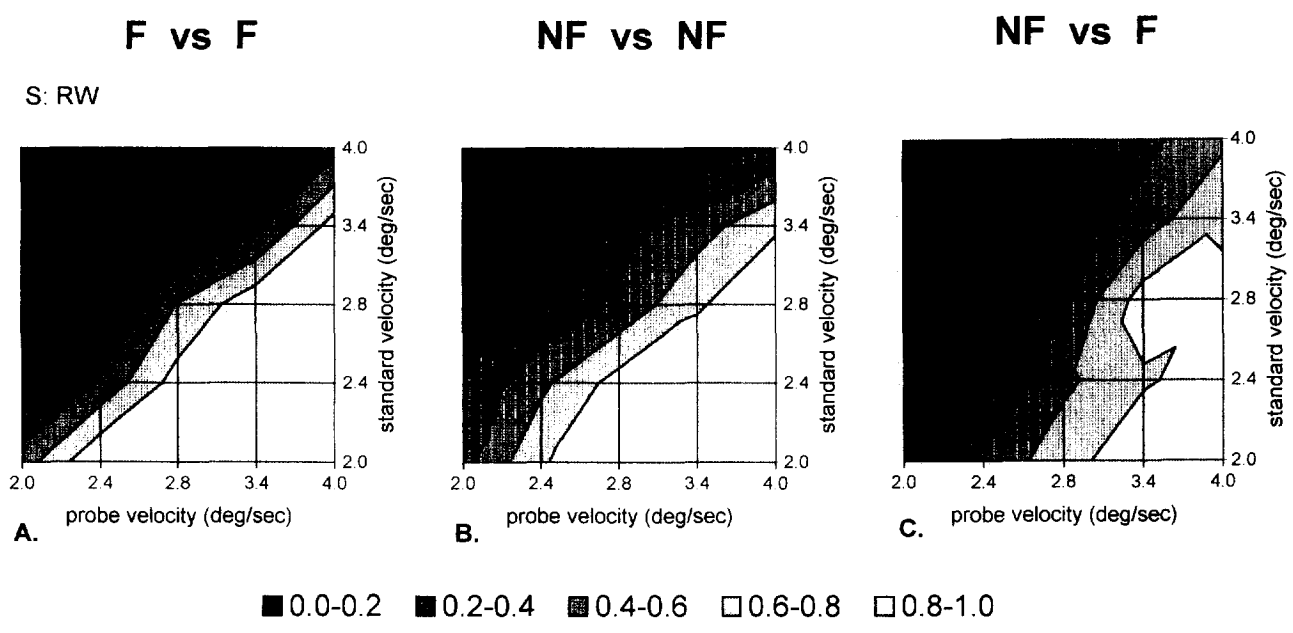

FIGURE 9. Psychometric functions (fraction of presentations in which the probe velocity is judged to be faster) for pairwise velocity comparisons between probe gratings of five velocities and standard gratings of five velocities, each in the range 2–4 deg/sec. (A) Comparison of Fourier gratings. (B) Comparison of non-Fourier gratings. (C) Comparison of non-Fourier (standard) and Fourier (probe) gratings; data replotted from Fig. 8. Contrasts as in Fig. 8. Subject: RW.

noticeable difference for the log velocity ratio. At a log velocity ratio of 0.47σ, 75% of judgments will be correct.

As the standard velocity increases parametrically from 2.0 to 4.0 deg/sec, the subjectively equal probe velocity also increases, as is indicated by a rightward shift of the psychometric functions. Fitting all of the data to Eq. (18) reveals that there is no significant deviation of the bias ratio b from 1 ($b = 1.041$, $\log b = 0.040$).

Figure 9 presents F vs F, NF vs NF, and NF vs F velocity comparisons for this subject as contour maps. These maps reveal an unexpected difference between the heterogeneous judgments (NF vs F) and the homogeneous judgments (F vs F and NF vs NF). If velocity judgments depended only on velocity ratio, then the contour lines (which represent constant frequency of judging the probe to be faster) would all have a slope of 45 deg (lines of constant velocity ratio). This expectation is met for F vs F judgments [Fig. 9(A)] and NF vs NF judgments [Fig. 9(B)]. However, for NF vs F judgments, the contour lines tend more towards the vertical, indicating that the velocity of the Fourier grating (the probe) is a more important determinant of the subject's response than the velocity of the non-Fourier grating (the standard). Additionally, the uncertainty σ was greater for the NF vs F condition ($\sigma = 0.18$) than for the F vs F condition ($\sigma = 0.07$) or the NF vs NF condition ($\sigma = 0.13$). Subject NW, who had a velocity bias ratio b slightly less than 1 ($b = 0.970$, $\log b = -0.030$), also showed a tilt of the contour lines towards vertical. The same pattern was seen for subject MC, for whom the bias ratio was essentially 1 ($b = 0.983$, $\log b = -0.017$).

Thus, even though there is no bias in comparisons of velocity of Fourier and non-Fourier gratings, subjects do appear to rely more heavily on the velocity of the Fourier grating in judging which is faster. Furthermore, there appears to be greater uncertainty in the judgment of the velocity of a non-Fourier grating than in the judgment of the velocity of a comparable Fourier grating (Table 1).

Experiment 4: Velocity judgments of Fourier gratings in noise

The above findings of subjectively equal velocities for F and NF gratings are consistent with those of Ledgeway & Smith (1995a), but appear inconsistent with a single-pathway scheme because of the difference in Weber fractions and the "tilt" of the contour lines of subjective equality [Fig. 9(C)]. However, a further test is required. This is because the nonlinear transformation T, when applied to a non-Fourier motion stimulus such as P_2, yields not only a drifting luminance grating but also non-directional energy ("noise"). Such non-directional components in the autocorrelation are produced by the action of a local nonlinearity on any non-Fourier motion stimulus, and not just the stimuli used in these studies. However, this noise is not present when T acts on a Fourier grating. The next experiment determines whether

TABLE 1. Summary of velocity comparisons and velocity discrimination for Fourier and non-Fourier gratings

Grating A	Grating B	Apparent velocity ratio (A/B)	Weber fraction
F	F	1.005	0.17
NF	NF	1.008	0.26
F	NF	1.005	0.35
F	F, low contrast	1.096	0.16
F, equivalent	F, equivalent	1.003	0.24
F	F, equivalent	0.949	0.26

Results are averages across three subjects.

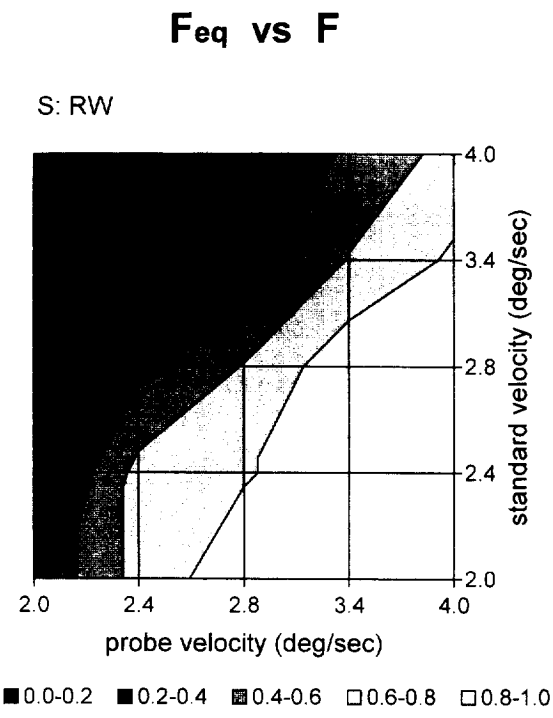

FIGURE 10. Psychometric functions (fraction of presentations in which the probe velocity is judged to be faster) for pairwise velocity comparisons between Fourier gratings of five velocities (probe) with "equivalent Fourier" gratings of five velocities (standard), each in the range 2–4 deg/sec. For details on the construction of the "equivalent Fourier" grating F_{eq}, see text. Subject: RW.

the apparent difference between the processing of a Fourier and a non-Fourier grating could be due to the "noise" inherent in a non-Fourier grating.

To test this possibility, we generated an "equivalent Fourier stimulus" F_{eq}, consisting of a standard Fourier grating and superimposed dynamic noise. The grating amplitude and noise amplitude in F_{eq} were uniquely determined by the joint constraints that $T(F_{eq})$ and $T(P_2)$ had identical Fourier motion signals, and identical noise power. For this calculation, P_2 was taken to be the NF grating of Experiment 3, and the nonlinearity T was given by Eq. (17), as suggested by the results of Experiment 2.

Figure 10 shows the results of F_{eq} vs F velocity judgments in a 5×5 design for subject RW. The main features of the NF vs F judgments are reproduced: there is no bias in velocity judgments ($b = 0.986$, $\log b = -0.014$), but the velocity of the F grating is weighted more strongly, as indicated by a tilt of the contour lines towards vertical. Furthermore, velocity judgments for F_{eq} vs F_{eq} were characterized by an uncertainty σ of 0.14 that was greater than that for F vs F judgments ($\sigma = 0.07$), but comparable to that for the NF vs NF judgments ($\sigma = 0.13$).

Results from Experiments 3 and 4 are summarized in Table 1. Apparent velocity ratios (derived from b) and Weber fractions (0.47σ, corresponding to the 75%-correct point) are averaged across subjects. There is no (<1%) subjective difference in the apparent velocity of Fourier and non-Fourier gratings equated for visibility. However, velocity comparisons have a greater uncertainty for the NF vs NF comparison than for the F vs F comparison, and a still greater uncertainty for the NF vs F comparison. These findings, which might appear to indicate that a separate pathway processes the NF grating, are also seen when the NF grating is replaced by an "equivalent" F grating in noise, F_{eq}. The uncertainty in the F vs F_{eq} comparison is not quite as large as in the NF vs F comparison. While this might indicate a need for a second pathway, it might also merely indicate errors in the estimation of T.

DISCUSSION

Summary of results

We defined an nth-order motion stimulus as one in which the underlying unidirectional motion is revealed only by an initial nonlinearity of formal order at least n, and showed how these stimuli may be constructed. For $n = 2$, 3 and 4, the constructed stimuli (P_2, P_3 and P_4) generated the perception of unidirectional motion. We determined contrast thresholds for motion detection for these stimuli alone and in the presence of added noise. We showed that these thresholds were consistent with each other and with measured thresholds for Fourier gratings, provided that the nonlinearity T preceding standard motion analysis was asymmetric and compressive. We identified differences in the perception of Fourier and second-order non-Fourier gratings of comparable spatial and temporal structure, and showed that velocity perception for non-Fourier gratings could be mimicked by a Fourier grating with added noise, in which the amplitudes of the grating and noise were calculated from the nonlinearity T.

It is now well-established that certain visual stimuli which lack directional motion energy are perceived as moving. The accepted working model for this phenomenon (e.g., Chubb & Sperling, 1989), as diagrammed by the scheme, is that of a nonlinear preprocessor, followed by standard motion analysis. However, the nature of the nonlinearity, the extent to which pathways which process non-Fourier motion are distinct from pathways which process Fourier motion, and the number of distinct non-Fourier pathways, are as yet unclear. We discuss our work with attention to these issues.

The nature of the nonlinearity

In general, non-Fourier motion stimuli will reveal unambiguous motion if they are subject to a stage of nonlinear processing prior to standard motion analysis. This nonlinear processing is not the very first stage of computation: prior linear spatial and/or temporal filtering is required (Chubb & Sperling, 1989). For most non-Fourier stimuli, the nature of the nonlinearity is not critical, as long as it is at least partially eliminates cancellation of negative and positive contrasts. Thus, quadratic (Emerson *et al.*, 1992; Lu & Sperling, 1995a), linear (Chubb & Sperling, 1989; Victor & Conte, 1992b), and other power laws ($\alpha = 0.73$) (Anderson *et al.*, 1991) have been proposed for the initial local nonlinearity.

Since full-wave and half-wave rectifiers differ only by a linear filter (i.e., a half-wave rectifier function can be synthesized by $T(p) = (p + |p|)/2$), it may be difficult to distinguish between these possibilities in the presence of linear spatiotemporal preprocessing. However, our results imply a non-integer exponent α for the contrast-scaling behavior of T, with a power near 0.5 providing the best account of the data. Furthermore, if T were symmetric, then there would be a smaller difference in thresholds for P_3 and P_4 than what we found.

Our method for identifying T is only an approximate one and is based on an assumed functional form. We cannot be confident of the shape of T in the low-contrast range (e.g., below 0.01). While there are undoubtedly other functional forms for T that would provide a satisfactory fit, the major features of our results imply that any such T would necessarily be both compressive and asymmetric.

Our model has a frank asymmetry: as proposed, increments and decrements of equal magnitude do not have the same effect on the output of the nonlinearity T. However, our data are consistent with the possibility that two pathways of the form exist [equation (10)], one with the proposed T, and one with its mirror-image $T'(x) = T(-x)$, provided that each of these signals is processed separately (Watt & Morgan, 1985).

Recently it has been proposed (Fleet & Langley, 1994) that non-Fourier motion can be thought of in terms of extraction of oriented lines or planes in the spatiotemporal Fourier transform of the stimulus which need not pass through the origin. However, this is inconsistent with our findings that the stimuli P_3 and P_4 have an unambiguous direction. The extraction of oriented (but perhaps displaced) lines or planes in Fourier space is tantamount to a purely quadratic nonlinearity preceding standard motion analysis (extraction of oriented *un*displaced lines or planes). This is because a quadratic nonlinearity applied to the stimulus merely convolves the Fourier domain representation of the stimulus with itself. Thus, a slanted line which does not pass through the origin, once convolved with itself, generates a longer line, at the same slope, which does pass through the origin—and thus, could be detected by standard motion analysis. Conversely, motion mechanisms which extract sloping lines in Fourier space will identify motion in any stimulus whose convolution with itself contains a sloping line through the origin. However, the Fourier representations of P_3 and P_4 do not contain any such sloping lines—this is equivalent to the statement that they require preprocessing by a nonlinearity of formal order higher than 2 to bring out motion by standard motion analysis. Thus, while the latent motion in P_3 and P_4 is essentially that of an envelope, this envelope is not manifest by sloping lines in Fourier space. Similarly, while dynamic occlusion typically results in the generation of non-Fourier motion signals (Fleet & Langley, 1994; Stoner & Albright, 1995), not all non-Fourier motion stimuli (for example, P_3 and P_4) correspond to dynamic occlusion.

Plaids

Plaid stimuli, which consist of two superimposed gratings moving in nonparallel directions, are perceived over a wide range of experimental conditions as a single coherent image, whose velocity is the unique velocity consistent with coherent motion of the plaid—the so-called intersection-of-constraints (IOC) velocity (Adelson & Movshon, 1982). Human observers' perceptions correspond only approximately to the IOC velocity (Stone, 1990; Yo & Wilson, 1992; Kim & Wilson, 1993). Heeger and coworkers (Heeger, 1987; Heeger & Simoncelli, 1995) have proposed detailed implementations of standard motion analysis based on a geometrical view of the stimulus representation in Fourier space, and several investigators (Movshon *et al.*, 1985; Wilson *et al.*, 1992) have suggested biological implementations of motion analysis. These models provide a reasonable account of a broad range of psychophysical phenomena.

These models generally do not include an early nonlinearity, but it is straightforward to understand the effects that such a nonlinearity will have. As described above, extraction of velocity from a two-dimensional stimulus amounts to determination of a plane in spatiotemporal Fourier space which contains the bulk of its motion energy. The IOC calculation yields the unique plane which contains the two vectors that correspond to the Fourier transforms of the gratings that constitute the plaid. The effect of a nonlinearity is to generate additional spatiotemporal Fourier components, which are sums and differences of the spatiotemporal frequencies that correspond to the original gratings. However, these new Fourier components are linear combinations of the two components of the plaid, and therefore lie in the same plane as the Fourier components of the original stimulus. Thus, they do not alter the constraints available to the IOC calculation. This is somewhat surprising, in that one might have expected that the presence or absence of a local nonlinearity (e.g., the extraction of "blobs" from crossed gratings) might make a difference in the information available for motion analysis.

Because non-Fourier pathway(s) do not generate any new constraints, this analysis does not reveal whether they have any role in the processing of plaid motion. However, the work of Derrington and coworkers (Derrington & Badcock, 1992; Derrington *et al.*, 1992) provides clear evidence in this regard. They used two-dimensional plaid stimuli in which the component motion was defined only by non-Fourier signals. These non-Fourier signals combined to provide a coherent motion of the plaid, in a manner similar to the combination of Fourier component motion signals in standard plaids. This is consistent with the idea that the nonlinearity that extracts non-Fourier motion occurs early in visual processing. On the other hand, the main determinants of whether gratings cohere, or moving stimuli appear to be rigid, appear to be higher-level influences (Nakayama & Silverman, 1985; Krauskopf & Farell, 1990; Shiffrar &

Pavel, 1991; Kooi *et al.*, 1992), rather than their Fourier or non-Fourier content as such.

How many motion pathways are necessary?

We have provided a quantitative account for the thresholds for the detection of motion direction in P_n in terms of a single nonlinear pathway that processes both Fourier and non-Fourier motion. Furthermore, this model accounts for the observation that velocity judgments for non-Fourier stimuli are veridical, but associated with a greater uncertainty. Adaptation and sensitivity studies provide independent psychophysical evidence that Fourier and non-Fourier pathways are processed by the same mechanism (Turano & Pantle, 1989; Turano, 1991; Ledgeway & Smith, 1995b), and this view is also in accord with direct physiological evidence (Albright, 1992). As in models for standard motion perception (e.g., Heeger & Simoncelli, 1995), we postulate that the basic computational unit is present at many spatial scales (and retinal eccentricities). Furthermore, although we did not examine this issue here, the effective balance of linear and nonlinear contributions [i.e., the parameter in Eq. (17)] may well vary at the extremes of spatial scale—for example, as the envelope spatial frequency becomes higher, the relative contribution of nonlinearities might be expected to decrease, simply because of optical and receptoral factors limiting the sensitivity of nonlinear subunits.

Most workers have concluded that Fourier and non-Fourier motion signals must be processed by separate pathways (e.g., Chubb & Sperling, 1989; Boulton & Baker, 1993a,b; Mather & Tunley, 1995; Lu & Sperling, 1995a). The specific functional form for the initial nonlinear stage that we postulate has implications, not all of which are obvious, for the way that Fourier and non-Fourier signals are processed and interact. We therefore re-examine many of these studies, to determine to what extent they are consistent with a one-pathway model.

There is ample evidence that the perception of motion in displays in which components move in large discrete steps is extracted by a pathway which is distinct from that which processes short-range motion (Braddick, 1974, 1980). Importantly, this long-range vs short-range distinction was identified in displays in which motion correspondence is driven by untransformed luminance (Fourier) signals. Motion driven by texture elements, depth, and "features" also appears to be processed by a pathway distinct from the pathway which processes short-range luminance-driven motion, on the basis of its slower dynamics, spatial coarseness, binocularity, and attentional modulation (Anstis, 1980; Braddick, 1980; Cavanagh, 1992; Lu & Sperling, 1995a,b). We too have found that stimuli constructed to contain textural tokens but balanced for features that could be extracted by a single nonlinear preprocessing stage generate a qualitatively different motion signal (Victor & Conte, 1990), which is substantially slower than processing of luminance-defined motion stimuli. Additionally, a single-intensity-based nonlinearity cannot account for interactions between color and motion, such as the apparent slowing of motion in near-isoluminant displays (Cavanagh *et al.*, 1984), the role of color in transparency (Krauskopf & Farell, 1990; Kooi *et al.*, 1992), or the role of color correspondence in disambiguation of motion (Papathomas *et al.*, 1991). Motion based on more local motion tokens (Zanker, 1993) also likely represents a kind of feature-based motion, but it is worth pointing out that some of "theta-motion" can indeed be extracted by a computation of the form [equation (10)], provided that the initial linear filter contains spatial and temporal components and the nonlinearity is not simply second-order.

Recognizing that motion based on feature extraction and long-range steps is processed separately, we therefore restrict our attention to perception of motion in achromatic stimuli presented continuously or in frame-by-frame displays with brief interframe intervals and short interframe displacements. Even within this restricted domain, there are many claims that two (or more) kinds of motion pathways are required to account for experimental data. These pathways are considered to be intrinsically different (i.e., distinguished by the presence of, or nature of, the nonlinear preprocessor), and not simply different in spatial scale. If the initial nonlinearity in the non-Fourier pathway (or pathways) were well-modeled by a quadratic transformation, then it would be relatively straightforward to determine whether this pathway existed in parallel to standard motion analysis. A more complex initial nonlinearity of the sort that we propose necessarily mixes linear and nonlinear components, because of its asymmetry. Furthermore, because the nonlinearity is not simply a quadratic one, it produces higher harmonics, and these may have non-intuitive effects. For both of these reasons, it is necessary to re-examine previous lines of evidence that appear to require multiple short-range motion pathways. Fundamentally, our claim of a single kind of pathway can never be proven by psychophysical or physiologic means; it can only be supported by parsimony and a lack of evidence to the contrary.

Stimuli with scale-dependent reversal in apparent motion

Chubb and Sperling's (1989) study of visual displays with conflicting Fourier and non-Fourier motion components provided some of the early evidence for separation of these two pathways. They found that such displays appear to have motion in the non-Fourier direction on close viewing, but in the Fourier direction when viewed from a greater distance. The shift from predominantly nonlinear preprocessing at short viewing distances to predominantly linear preprocessing at large distances is, however, consistent with a single initial filter with both linear and nonlinear components. Consider a receptive field element which subtends a fixed visual angle and whose nonlinear nature consists of partial rectification of the form [equation (16)]. At short viewing distances, this receptive field element might encompass only a single stimulus pixel, and thus its nonlinear nature would be directly manifest in its output. However, at longer

viewing distances, it would subtend multiple stimulus pixels, many of which would be uncorrelated. These uncorrelated pixels would act as a source of noise, and thus reduce the apparent effects of the nonlinearity, as discussed above in connection with the effects of spatial summation on the estimate of T. That is, a single pathway with linear filtering followed by a nonlinearity can appear to be roughly linear for high stimulus densities, but highly nonlinear for low stimulus densities.

The nature of the "Γ" stimulus used by Chubb & Sperling (1989) suggests that there is at least partial full-wave rectification in the initial nonlinearity; i.e., that the nonlinearity is of the form [equation (16)] with a somewhat negative value of g. Although we have used $g = 0$, this estimate was derived from an assumption that there was no spatial filtering prior to the initial nonlinear stage. As we have pointed out, unmodelled spatial pooling prior to the nonlinearity biases the estimate of the form of P towards linearity. Thus, our data are consistent with spatial pooling along with a somewhat negative value for g.

Evidence from micropattern displays

Boulton & Baker (1993a,b) examined the maximum displacement for apparent motion (D_{max}) for two-frame displays composed of Gabor micropatterns. They found that under conditions of high micropattern density or brief interstimulus intervals, psychophysical performance was consistent with the Fourier components of the stimulus, but under conditions of low density in space or time, performance was best explained on the basis of a second, highly nonlinear, mechanism. This argument that the change in the apparent nature of processing with spatial scale implies separation of motion pathways for Fourier and non-Fourier motion is akin to that of Chubb & Sperling (1989), and again overlooks the expected behavior (apparent linearization) of a nonlinear filter confronted with multiple uncorrelated inputs.

Evidence from random-dot kinematograms

Mather & Tunley (1995) used a clever random-dot kinematogram display to examine characteristics of motion processing. Even though their stimuli contained directional motion energy without a nonlinear preprocessor, they showed that rectification was required to account for the robust perception of motion despite contrast inversion. They posited that first-order motion was processed by a half-wave rectifying pathway, and argued that a separate full-wave rectifying pathway was required to prevent intrusion of reversed-phi motion. However, this second conclusion was based on an assumption that direction judgments were based on motion energy at low spatiotemporal frequencies (their Fig. 6); without this assumption, half-wave rectification would suffice. Furthermore, their argument does not exclude a single pathway based on an asymmetric full-wave rectifier. This is provided by the form [equation (16)] with a somewhat negative value of g, and is consistent with our findings, provided that spatial summation is included in the preprocessing stage.

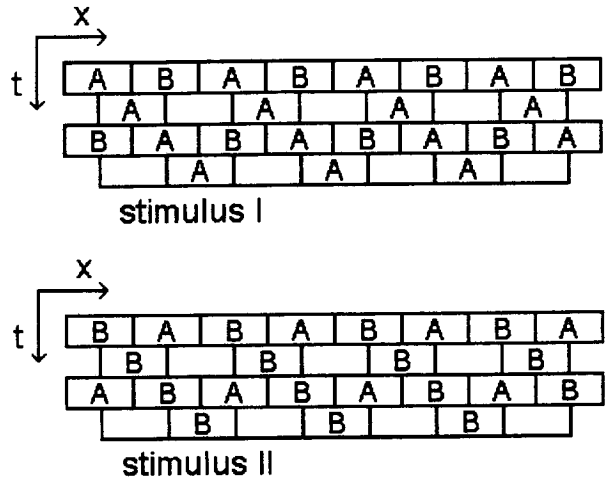

FIGURE 11. A diagram of stimuli used in the "transition-invariance" technique (Werkhoven *et al.*, 1993).

Evidence from interleaved apparent-motion displays

"Transition-invariance" is a powerful technique developed by Chubb and coworkers (Werkhoven *et al.*, 1993) to determine whether a single class of detectors can account for detection of motion in apparent-motion stimuli. This approach is based on the apparent motion stimuli whose space–time diagrams are shown in Fig. 11. In each stimulus, there is the possibility to see apparent motion to the right or to the left. The observer adjusts some parameter of the token A until motion appears ambiguous. In stimulus I, this equates the apparent strength of the homogeneous motion path A→A→A→A →... with that of the heterogeneous motion path B→A→B→A→...; in stimulus II, this equates the apparent strength of the homogeneous motion path B→B→B→B→... with that of the heterogeneous motion path A→B→A→B→.... If motion balance is achieved at the same parameter setting for token A, then A and B are said to obey "transition invariance".

Assuming that standard motion analysis is characterized by crosscorrelation, motion balance in stimulus I implies that $T(A)T(A) = T(B)T(A)$, and thus $T(A) = T(B)$. This implies that $T(B)T(B) = T(A)T(B)$, which in turn implies that motion balance is present in stimulus II. Thus it would seem that in any single-pathway model, transition-invariance must hold. However, subtle but definite violations of transition-invariance for stimuli of the sort shown in Fig. 11 have been found (McGowan & Chubb, 1995; Papathomas *et al.*, 1995). This would appear to indicate that perceived motion in first- and second-order stimuli could not be accounted for by a single pathway.

There are, however, several problems with this argument. One problem is that it may not be valid to assume that processing at each successive time interval is independent. Since spatiotemporal filtering (at the very least, in the outer retina) necessarily precedes any

nonlinearity, the local response to the alternate ABABAB rows will not be identical in the two stimuli—in one case, it follows a row of As; in the other, it follows a row of Bs. A related issue is that the two displays differ in overall spatiotemporal frequency content: the spatiotemporal frequency content of stimulus I is dominated by that of A, and the spatiotemporal frequency content of stimulus II is dominated by that of B. As indicated below, the processes by which motion information is integrated across different spatiotemporal frequencies are not as yet clear, and thus, differences in the overall spatiotemporal frequency content could contribute to differences in the equivalence points.

Yet a third, and perhaps most interesting, problem with this argument is raised by the work of Chubb & Darcy (1995). At the "standard motion analysis" stage, two signals (say a and b) derived by sampling the inputs at points separated in space and time are compared by a cross-correlator $C(a, b)$. In motion analysis based on a Reichardt (1961) model or any of its computational equivalents (e.g., van Santen & Sperling, 1984), this cross-correlator is assumed to be strict multiplication: $C(a, b) = ab$. Chubb & Darcy (1995) point out that motion signals will be generated even if this cross-correlator need not strictly be multiplication, and have devised a psychophysical approach to investigate C directly based on two-frame displays. This investigation revealed that C is not symmetric, and furthermore, the symmetric component of C is not even multiplicative. Additionally, there is some recent direct physiological evidence (Kontsevich & Ferster, 1995) that the neural implementation of the Reichardt detector may indeed be characterized by an asymmetric cross-correlator. These deviations permit violations of transition-invariance, even in a one-pathway model. Suppose that a represents the result of the initial nonlinearity acting on token A, and b represents the result of the initial nonlinearity acting on token B. The condition for motion balance in stimulus I is $2C(a, a) = C(a, b) + C(b, a)$. The condition for motion balance in stimulus II is $2C(b, b) = C(a, b) + C(b, a)$. If C were simply a product, then either equation would imply that $a = b$, and hence, that the other equation held as well. But as Chubb & Darcy (1995) have shown, C has a more general form, and probably includes terms such as a^2b. With these terms, neither motion-balance condition necessarily implies that $a = b$, and neither motion-balance condition necessarily implies the other one. This allows violation of transition-invariance within the context of a single-pathway model.

Evidence from superimposed Fourier and non-Fourier motion displays

Lu & Sperling (1995a, b) identified three motion systems: a first-order motion system (standard motion analysis), a second-order motion system (nonlinear preprocessing followed by standard motion analysis), and a "third-order" system (feature-tracking). The second-order system shared many of the attributes that served to distinguish the first-order system from the feature-tracking system, including rapid dynamics, high sensitivity, monocularity, and resistance to pedestals. The main evidence that the first-order and the second-order systems were not identical comes from an experiment in which they examined direction judgments for superimposed Fourier and non-Fourier gratings as a function of relative spatial phase (their Experiment 4). They argued that if such judgments were mediated by a single combined pathway, then there should be a dependence of psychophysical performance on relative phase. (For example, two standard drifting gratings, when superimposed in antiphase, generate a spatially uniform display and thus no motion signal.) Since only a small phase dependence was observed, they reasoned that these two pathways are independent.

We have simulated this experiment with an initial nonlinearity corresponding to Eq. (17). For a stimulus consisting of a superimposed Fourier and non-Fourier grating in which the envelope spatiotemporal frequency of the non-Fourier grating matches the spatiotemporal frequency of the Fourier grating, motion energy varies by 16% (average fractional deviation) with relative spatial phase [corresponding to Lu & Sperling, 1995a; Fig. 10(a, b)]. When the envelope spatiotemporal frequency of the non-Fourier grating is twice that of the Fourier grating, motion energy varies by 7% (average fractional deviation) with relative spatial phase [corresponding to Lu & Sperling, 1995a; Fig. 10(c, d)]. While the simulations indeed reveal that there is a dependence on relative phase, this dependence is surprisingly small. The unexpectedly small size of the phase dependence is a consequence of the nature of the nonlinearity we propose. In contrast, a full-wave rectifier leads to phase-dependent interactions of 24% (NF grating whose envelope spatial frequency is equal to that of the F grating) and 43% (NF grating whose envelope spatial frequency is twice that of the F grating). A purely quadratic nonlinearity would lead to phase-dependent interactions of 4% and 58% in these two cases.

These simulations thus indicate that an asymmetric power-law rectifier is consistent with the small phase dependence observed by Lu & Sperling (1995a). Not only is the expected phase dependence of motion energy small, but also there are two other factors which further reduce the likelihood that it would have been observed psychophysically. The authors measured fraction of correct judgments, not motion energy, and the measurements were made in the range of 85–95%-correct performance. In this range, the fraction correct is likely to be a compressive function of motion energy. Furthermore, the Fourier and non-Fourier gratings were presented in alternate rows of the raster display; this spatial separation would reduce interactions among the two kinds of gratings simply because they might tend to stimulate separate detectors.

Fourier and non-Fourier gratings: what is required for equivalence?

Although many investigators have embraced the

concept that non-Fourier gratings are processed by a pathway in which a preliminary nonlinearity precedes standard motion analysis, they have often assumed that one can investigate the relationship of these two pathways by asking whether the non-Fourier grating is equivalent, in some sense, to the envelope that is extracted by the nonlinearity (e.g., Albright, 1992; Solomon & Sperling, 1994; Ledgeway & Smith, 1995a). The problem with this approach is that an initial nonlinearity will not only generate the envelope, but it will also generate other spatiotemporal frequencies—particularly if the nonlinearity has higher-order components, such as the form [equation (17)]. Many of these additional Fourier components will not contain motion information, and thus behave like a mask. That is, a single-pathway model does not predict that a non-Fourier grating will behave in the same way as its envelope, but rather, that a non-Fourier grating will behave in the same way as a Fourier grating plus a noise mask, provided that these stimuli, after nonlinear preprocessing, have the same spatiotemporal spectra.

In Experiment 4, we have shown that explicit inclusion of this mask can account for much of the apparent difference between the perception of a non-Fourier stimulus and the perception of its Fourier envelope. We were able to construct this "equivalent" stimulus because the stimulus P_2 has a simple structure and we assumed a definite form for the nonlinearity. For other non-Fourier stimuli (Chubb & Sperling, 1988; Petersik, 1995), the effective mask may be complex in spatiotemporal structure, and it may or may not be possible to create "equivalent" stimuli which contain Fourier motion, yet provide the same spatiotemporal components following nonlinear transformation. Furthermore, in experiments in which the non-Fourier grating is presented along with a Fourier grating, the additional spatiotemporal components generated by the nonlinearity will depend on the Fourier grating as well. Finally, interpretation of responses to Fourier motion stimuli necessarily entail consideration of the additional spatiotemporal components generated by the nonlinearities involved in the processing of non-Fourier motion.

Because of these complications, dissection of Fourier and non-Fourier stimuli requires a thorough understanding of how the visual system integrates motion energy across spatial frequencies (Ramachandran & Anstis, 1983; Zhang *et al.*, 1993; Nishida *et al.*, 1995; Smith & Derrington, 1995), how contrast is used (Thompson, 1982; Stone *et al.*, 1990; Stone & Thompson, 1992; Castet *et al.*, 1993), and how ambiguous stimuli with complex spectra are interpreted as coherent, transparent, (Adelson & Movshon, 1982; Movshon *et al.*, 1985; Ferrera & Wilson, 1990; Stoner *et al.*, 1990; Stoner & Albright, 1992; Victor & Conte, 1992a; Wilson *et al.*, 1992; Kim & Wilson, 1993; Wilson & Kim, 1994) or non-rigid (Shiffrar & Pavel, 1991; Yo & Wilson, 1992). These considerations, which are largely independent of whether separate Fourier and non-Fourier pathways exist, make it problematic to interpret superposition experiments as straightforward evidence for the presence of multiple short-range motion pathways (Solomon & Sperling, 1994).

Given these complexities, it is reasonable to wonder whether motion analysis, which entails complex interactions across spatial and temporal frequencies, would take a simpler form if analyzed in the spatiotemporal domain rather than in the Fourier domain. Many workers (e.g., Fennema & Thompson, 1979; Sobey & Srinivasan, 1991; Heeger & Simoncelli, 1995) have taken the alternative view, and proposed models for motion processing based on the extraction of a local spatiotemporal gradient. Such models will necessarily entail interactions across spatial frequencies. Johnston and Clifford have elaborated this view, and have shown that a unified model of this sort correctly predicts a variety of apparent motion illusions (Johnston & Clifford, 1995a) as well as some aspects of interactions between contrast and perceived velocity (Johnston & Clifford, 1995b). Furthermore, their model (Johnston & Clifford, 1995b) includes rectification at the front end, which is introduced to improve performance for luminance grating stimuli and for contrast-modulated gratings alike. Our work is consistent with this kind of model, provided that the rectification is not a simple square-law device. Most likely, the form of the rectification is not critical to its purpose. Additionally, we echo Johnston and Clifford's view (1995b) that the requirement for multiple motion mechanisms (Kim & Wilson, 1993; Chubb & Sperling, 1988, 1989; McGowan & Chubb, 1995; Solomon & Sperling, 1994) at multiple spatial scales engenders the problem of how these multiple signals are then integrated.

REFERENCES

Adelson, E. H. & Movshon, J. A. (1982). Phenomenal coherence of moving visual patterns. *Nature, 300*, 523–525.

Albright, T. D. (1992). Form-cue invariant motion processing in primate visual cortex. *Science, 255*, 1141–1143.

Anderson, S. J., Burr, D. C. & Morrone, M. C. (1991). Two-dimensional spatial and spatial-frequency selectivity of motion-sensitive mechanisms in human vision. *Journal of the Optical Society of America A, 8*, 1340–1351.

Anstis, S. M. (1980). The perception of apparent movement. *Philosophical Transactions of the Royal Society of London B, 290*, 153–168.

Boulton, J. C. & Baker, C. L. Jr. (1993a) Different parameters control motion perception above and below a critical density. *Vision Research, 33*, 1803–1811.

Boulton, J. C. & Baker, C. L. Jr. (1993b) Dependence on stimulus onset asynchrony in apparent motion: evidence for two mechanisms. *Vision Research, 33*, 2013–2019.

Braddick, O. (1974). A short-range process in apparent motion. *Vision Research, 14*, 519–529.

Braddick, O. (1980). Low-level and high-level processes in apparent motion. *Philosophical Transactions of the Royal Society of London B, 290*, 137–151.

Castet, E., Lorenceau, J., Shiffrar, M. & Bonnet, C. (1993). Perceived speed of moving lines depends on orientation, length, speed and luminance. *Vision Research, 33*, 1921–1936.

Cavanagh, P. (1992). Attention-based motion perception. *Science, 257*, 1563–1565.

Cavanagh, P., Tyler, C. W. & Favreau, O. E. (1984). Perceived

velocity of moving chromatic gratings. *Journal of the Optical Society of America A, 1*, 893–899.

Chubb, C. & Darcy, U. (1995). The short range motion matching strength function measured using histogram contrast analysis. *Investigative Ophthalmology and Visual Science, 36 suppl.*, 395.

Chubb, C. & Sperling, G. (1988). Drift-balanced random stimuli: a general basis for studying non-Fourier motion perception. *Journal of the Optical Society of America A, 5*, 1986–2006.

Chubb, C. & Sperling, G. (1989). Two motion perception mechanisms revealed through distance-driven reversal of apparent motion. *Proceedings of the National Academy of Sciences USA, 86*, 2985–2989.

Derrington, A. M. & Badcock, D. R. (1992). Two-stage analysis of the motion of 2-dimensional patterns: What is the first stage? *Vision Research, 32*, 691–698.

Derrington, A. M., Badcock, D. R. & Holroyd, S. A. (1992). Analysis of the motion of 2-dimensional patterns: evidence for a second-order process. *Vision Research, 32*, 699–707.

Emerson, R. C., Bergen, J. R. & Adelson, E. H. (1992). Directionally selective complex cells and the computation of motion energy in cat visual cortex. *Vision Research, 32*, 203–218.

Enroth-Cugell, C. & Robson, J. G. (1966). The contrast sensitivity of retinal ganglion cells of the cat. *Journal of Physiology, 187*, 517–552.

Fennema, C. L. & Thompson, W. B. (1979). Velocity determination in scenes containing several moving objects. *Computer Graphics and Image Processing, 9*, 301–305.

Ferrera, V. P. & Wilson, H. R. (1990). Perceived direction of moving two-dimensional patterns. *Vision Research, 30*, 273–287.

Fleet, D. J. & Langley, K. (1994). Computational analysis of non-Fourier motion. *Vision Research, 34*, 3057–3079.

Heeger, D. J. (1987). Model for the extraction of image flow. *Journal of the Optical Society of America A, 4*, 1455–1471.

Heeger, D. J. & Simoncelli, E. P. (1995). Model of visual motion sensing. In Harris, L. & Jenkins, M. (Eds). *Spatial vision in humans and robots*. New York: Cambridge University Press.

Hochstein, S. & Shapley, R. M. (1976). Linear and nonlinear spatial subunits in Y cat retinal ganglion cells. *Journal of Physiology, 262*, 265–284.

Johnston, A. & Clifford, C. W. G. (1995a) A unified account of three apparent motion illusions. *Vision Research, 35*, 1109–1123.

Johnston, A. & Clifford, C. W. G. (1995b) Perceived motion of contrast-modulated gratings: predictions of the Multi-Channel Gradient Model and the role of full-wave rectification. *Vision Research, 35*, 1771–1783.

Kim, J. & Wilson, H. R. (1993). Dependence of plaid motion coherence on component grating directions. *Vision Research, 33*, 2479–2489.

Kontsevich, L. L. & Ferster, D. (1995). The internal structure of cortical motion detectors. *Investigative Ophthalmology and Visual Science, 36 suppl.*, 692.

Kooi, F. L., de Valois, K. K., Switkes, E. & Grosof, D. H. (1992). Higher-order factors influencing the perception of sliding and coherence of a plaid. *Perception, 21*, 583–598.

Krauskopf, J. & Farell, B. (1990). Influence of colour on the perception of coherent motion. *Nature, 348*, 328–331.

Ledgeway, T. & Smith, A. T. (1995a) The perceived speed of second-order motion and its dependence on stimulus contrast. *Vision Research, 35*, 1421–1434.

Ledgeway, T. & Smith, A. T. (1995b) Effects of adaptation to second-order motion on perceived speed. *Investigative Ophthalmology and Visual Science, 36 suppl.*, 53.

Lu, Z.-L. & Sperling, G. (1995a) The functional architecture of human visual motion perception. *Vision Research, 35*, 2697–2772.

Lu, Z.-L. & Sperling, G. (1995b) Attention-generated apparent motion. *Nature, 377*, 237–239.

Mather, G. & Tunley, H. (1995). Motion detection in interleaved random dot patterns: evidence for a rectifying nonlinearity preceding motion analysis. *Vision Research, 35*, 2117–2125.

McGowan, J. W. & Chubb, C. (1995). Modelling a second texture-defined motion channel. *Investigative Ophthalmology and Visual Science, 36 suppl.*, 51.

Milkman, N., Schick, G., Rossetto, M., Ratliff, F., Shapley, R. & Victor, J. D. (1980). A two-dimensional computer-controlled visual stimulator. *Behavior Research Methods and Instrumentation, 12*, 283–292.

Movshon, J. A., Adelson, E. H., Gizzi, M. S. & Newsome, W. T. (1985). The analysis of moving visual patterns. In Chagas, C., Gattass, R. & Gross, C. (Suppl. 11), *Pattern recognition mechanisms, experimental brain research*. Berlin: Springer.

Nakayama, K. & Silverman, G. H. (1985). Detection and discrimination of sinusoidal grating displacements. *Journal of the Optical Society of America A, 2*, 267–274.

Naiman, A. C. & Makous, W. (1992). Spatial non-linearities of grayscale CRT pixels. *SPIE Human Vision, Visual Processing, and Digital Display, 1666*, 41–46.

Nishida, S., Yanagi, J. & Sato, T. (1995). Motion assimilation and contrast in superimposed gratings: effects of spatiotemporal frequency. *Investigative Ophthalmology and Visual Science, 36 suppl.*, 56.

Papathomas, T. V., Gorea, A. & Chubb, C. (1995). Separate 1st-order and 2nd order motion systems or a single motion system? *Investigative Ophthalmology and Visual Science, 36 suppl.*, 51.

Papathomas, T. V., Gorea, A. & Julesz, B. (1991). Two carriers for motion perception: color and luminance. *Vision Research, 31*, 1883–1891.

Pelli, D. & Zhang, L. (1991). Accurate control of contrast on microcomputer displays. *Vision Research, 31*, 1337–1350.

Petersik, J. (1995). A comparison of varieties of "second-order" motion. *Vision Research, 35*, 507–517.

Ramachandran, V. S. & Anstis, S. M. (1983). Perceptual organization in moving patterns. *Nature, 304*, 529–531.

Reichardt, W. (1961). Autocorrelation, a principle for the evaluation of sensory information by the central nervous system. In Rosenbluth, W. A. (Ed.), Sensory communication. Wiley, New York.

Shiffrar, M. & Pavel, M. (1991). Percepts of rigid motion within and across apertures. *Journal of Experimental Psychology, 17*, 749–761.

Smith, D. R. R. & Derrington, A. M. (1995). Modifying perceived speed: temporal frequency and orientation effects. *Investigative Ophthalmology and Visual Science, 36 suppl.*, 53.

Sobey, P. & Srinivasan, M. V. (1991). Measurement of optical flow by a generalized gradient scheme. *Journal of the Optical Society of America A, 8*, 1488–1498.

Solomon, J. A. & Sperling, G. (1994). Full-wave and half-wave rectification in second-order motion perception. *Vision Research, 34*, 2239–2258.

Spekreijse, H. & Oosting, J. (1970). A method for analyzing and synthesizing nonlinear systems. *Kybernetik, 7*, 23–31.

Stone, L. S. (1990). Precision in the perception of plaid motion. *Investigative Ophthalmology and Visual Science, 31 suppl.*, 172.

Stone, L. S. & Thompson, P. (1992). Human speed perception is contrast dependent. *Vision Research, 32*, 1535–1549.

Stone, L. S., Watson, A. B. & Mulligan, J. B. (1990). Effect of contrast on the perceived direction of a moving plaid. *Vision Research, 30*, 1049–1067.

Stoner, G. R. & Albright, T. D. (1992). Motion coherency rules are form-cue invariant. *Vision Research, 32*, 465–475.

Stoner, G. R. & Albright, T. D. (1995). Depth from occlusion and non-Fourier motion. *Society for Neuroscience Abstracts, 21*, 511.

Stoner, G. R., Albright, T. D. & Ramachandran, V. S. (1990). Transparency and coherence in human motion perception. *Nature, 344*, 153–155.

Taub, E. & Victor, J. D. (1993). Higher-order non-Fourier motion stimuli and nonlinearity in early motion processing. *Investigative Ophthalmology and Visual Science, 34 suppl.*, 1028.

Thompson, P. (1982). Perceived rate of movement depends on contrast. *Vision Research, 22*, 377–380.

Turano, K. (1991). Evidence for a common motion mechanism of luminance- and contrast-modulated patterns: selective adaptation. *Perception, 20*, 455–466.

Turano, K. & Pantle, A. (1989). On the mechanism that encodes the

movement of contrast variations: velocity discrimination. *Vision Research, 29*, 207–221.

van Santen, J. P. H. & Sperling, G. (1984). Temporal covariance model of human motion perception. *Journal of the Optical Society of America A, 1*, 451–473.

Victor, J. D. & Conte, M. M. (1990). Motion mechanisms have only limited access to form information. *Vision Research, 30*, 289–301.

Victor, J. D. & Conte, M. M. (1992a) Coherence and transparency of moving plaids composed of Fourier and non-Fourier gratings. *Perception and Psychophysics, 52*, 403–414.

Victor, J. D. & Conte, M. M. (1992b) Evoked potential and psychophysical analysis of Fourier and non-Fourier motion mechanisms. *Visual Neuroscience, 9*, 105–123.

Watt, R. J. & Morgan, M. J. (1985). A theory of the primitive spatial code in human vision. *Vision Research, 25*, 1661–1674.

Werkhoven, P., Sperling, G. & Chubb, C. (1993). The dimensionality of texture-defined motion: a single channel theory. *Vision Research, 33*, 463–485.

Wilson, H. R., Ferrera, V. P. & Yo, C. (1992). A psychophysically motivated model for two-dimensional motion perception. *Visual Neuroscience, 9*, 79–98.

Wilson, H. R. & Kim, J. (1994). A model for motion coherence and transparency. *Visual Neuroscience, 11*, 1205–1219.

Witt, R., Conte, M. M., Waran, M. & Victor, J. D. (1994). Perceived velocity of Fourier and non-Fourier stimuli. *Investigative Ophthalmology and Visual Science, 35 suppl.*, 1269.

Yo, C. & Wilson, H. R. (1992). Perceived direction of moving two-dimensional plaids depends on duration, contrast, and eccentricity. *Vision Research, 32*, 135–147.

Zanker, J. M. (1993). Theta motion: a paradoxical stimulus to explore higher order motion extraction. *Vision Research, 33*, 553–569.

Zhang, J. & Yeh, S.-L, De Valois, K.K. (1993). Motion contrast and motion integration. *Vision Research, 33*, 2721–2732.

Acknowledgements—This material was presented in part at the Association for Research in Vision and Ophthalmology annual meetings in 1993 and 1994. We thank Manisha Waran and Rochelle Witt for their assistance, and gratefully acknowledge the Frontiers support received by Rochelle Witt. This work was supported by NIH grant EY7977 to J. Victor.